Advanced Response Surface Modeling of Ares I Roll Control Jet Aerodynamic Interactions

Noah M. Favaregh*
Analytical Mechanics Associates, Hampton, VA, 23666

The Ares I rocket uses roll control jets. These jets have aerodynamic implications as they impinge on the surface and protuberances of the vehicle. The jet interaction on the body can cause an amplification or a reduction of the rolling moment produced by the jet itself, either increasing the jet effectiveness or creating an adverse effect. A design of experiments test was planned and carried out using computation fluid dynamics, and a subsequent response surface analysis ensued on the available data to characterize the jet interaction across the ascent portion of the Ares I flight envelope. Four response surface schemes were compared including a single response surface covering the entire design space, separate sector responses that did not overlap, continuously overlapping surfaces, and recursive weighted response surfaces. These surfaces were evaluated on traditional statistical metrics as well as visual inspection. Validation of the recursive weighted response surface was performed using additionally available data at off-design point locations.

Nomenclature

A103	=	Ares A103 OML, previous configuration
A106	=	Ares A106 OML, current configuration
AOA	=	total angle of attack, missile axis, deg
BTM	=	booster tumble motor
CFD	=	computational fluid dynamics
C_l	=	rolling moment coefficient
deg	=	degrees
DOE	=	design of experiments
DOF	=	degrees of freedom
FTV	=	flight test vehicle OML configuration
E	=	estimate
E_J	=	jet efficiency factor
ft	=	foot
JI	=	jet interaction
k	=	number of regressors
L	=	least squares operator
LS	=	least squares
lb	=	pounds force
M	=	Mach number
n	=	number of observations
OML	=	outer mold line
P_{ATM}	=	atmospheric pressure, lb/ft^2
phi	=	roll angle, deg
PRESS	=	prediction error sum of squares
R	=	Rankine
R^2	=	coefficient of multiple determination.
Re	=	Reynold's number
RoCS	=	roll control system

* Senior Project Engineer, AeroSciences, 303 Butler Farm Rd., Hampton, VA 23666, AIAA Member.

RSM = response surface methodology
RWSR = recursive weighted sector regression
s = sample standard deviation
T = temperature, R
var = variance
VIF = variable inflation factors
w = weighting variable
W = weighting matrix
WR = weighting ratio
x = regressor variable
X = regressor matrix
y = system response
$\hat{y}$ = estimated system response
α_T = total angle of attack, missile axis, deg
b = least squares regressor coefficient estimate
β = regressor coefficient
ΔC_l = change in rolling moment due to jet interaction
ΔC_p = change in pressure coefficient
ε = residual
Σ = summation
φ = roll orientation, deg
γ = gas constant
ρ = air density, lb/ft^3
σ = population standard deviation
ψ = influence function

Subscripts
i, j, m = indexing variables
JI = jet interaction
RoCS = roll control system activated

Superscripts
T = matrix transpose
–1 = inverse matrix
^ = estimated

I. Introduction

DESIGN of experiments (DOE) and response surface methodology (RSM) have been well understood and practiced in fields such as industrial engineering, automotive engineering, and agriculture for many decades. For the past 25 years it has made a slow but needed infusion into aerospace research due in large part to the works of DeLoach[1–3], Landman[4–6], and Parker[7–9]. Unfortunately, it has been used very seldom in production cycles for math critical models of air vehicles where many still view the use of DOE in aerospace as a research project. The tests needed for math critical models of air vehicles consists of wind tunnel experiments, computational fluid dynamics (CFD) evaluations, and flight tests. These are areas of great potential for an improvement in information efficiency and accuracy due to the large amount of testing required. Air vehicle aerodynamics are notorious for being highly nonlinear, especially for body to body interactions, induced airflow to body interactions, protuberance interactions, and extreme flight envelope conditions such as high angle of attack or sideslip. The application of DOE and RSM to capture highly nonlinear aerodynamics will improve the efficiency and accuracy of these complex tests.

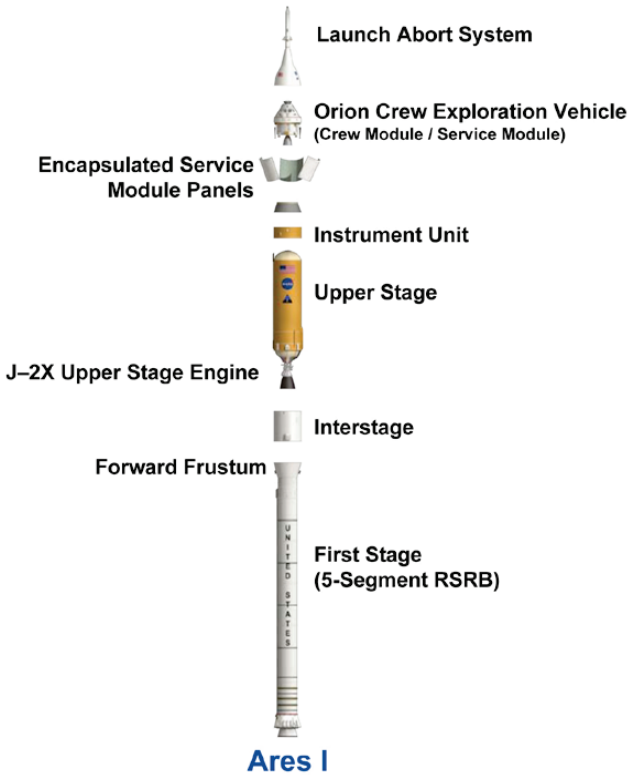

Figure 1: Ares I major components.

For this research, the problem is to characterize the roll control jet interaction on the body of the Ares I rocket as accurately and efficiently as possible, covering the flight envelope of subsonic through supersonic speeds, and all possible angles of attack and roll orientations. This is a difficult problem in general to solve because it is experimentally very challenging to model the Reynold's number (Re) and jet expansion physics. Therefore the interaction must be characterized by CFD and these results must be relied upon without validation until actual flight data becomes available. The CFD must use very fine grid models, 50 million grid points in this study, becoming computationally expensive. The Ares I flight envelope is also very expansive, requiring a large but locally accurate design space and model to cover all necessary conditions. Figure 1 shows a breakdown of the major vehicle components.

Filling the design space can be done in several ways, one of which is to choose cardinal design Mach, angle of attack, and roll orientations and take a data point at each design locale. At this point there would be no modeling as every intersection along these cardinal conditions would contain a data point. A problem associated with this approach is the commonly used assumption that between the cardinal conditions the response is completely linear and there is no measure of the variation from linearity. If a validation point is used and the linear assumption is not valid, a large number of points would need to be added to capture the variation and keep the database "square". On the other hand, when performed as response surfaces based on an orthogonal and balanced array, all linear, nonlinear, and factor interactions can be captured with fewer points than including all cardinal intersections. During testing, it is useful to evaluate the data in steps so that the test can be redirected or modified if necessary, possibly reducing or increasing the number of points needed, but in the fast pace of the Ares I design cycle CFD evaluation, this was not a possibility. In this study, the designers assumed, based on previous data, that second order designs in sectored design spaces would capture all physics needed for model adequacy of the jet interaction.

Jet interaction research has been performed on jets acting normal to cylindrical bodies and flat plates[10-17]. This type of research most commonly investigates normal force and pitching moment effectiveness for abrupt control changes, while the current study characterizes tangential jet interactions. Jet efficiency parameters are commonly used as a metric to understand the effect of the jet on the body, but in this case the change in rolling moment was used.

II. Vehicle and System Description

The Ares I rocket is the crewed launch vehicle being developed by NASA as a Space Shuttle replacement under the Constellation Program. It is an in-line, two stage rocket. The first stage is a five-segment reusable solid rocket booster that propels the vehicle to a speed of Mach 5.7 and an altitude of about 35.5 miles where it then separates and reenters the atmosphere. The upper stage then powers the Orion Crew Exploration Vehicle using a J-2X engine fueled by liquid oxygen and liquid hydrogen to an altitude of about 80 miles where the Orion module separates and climbs to 185 miles for a circular orbit above Earth[18].

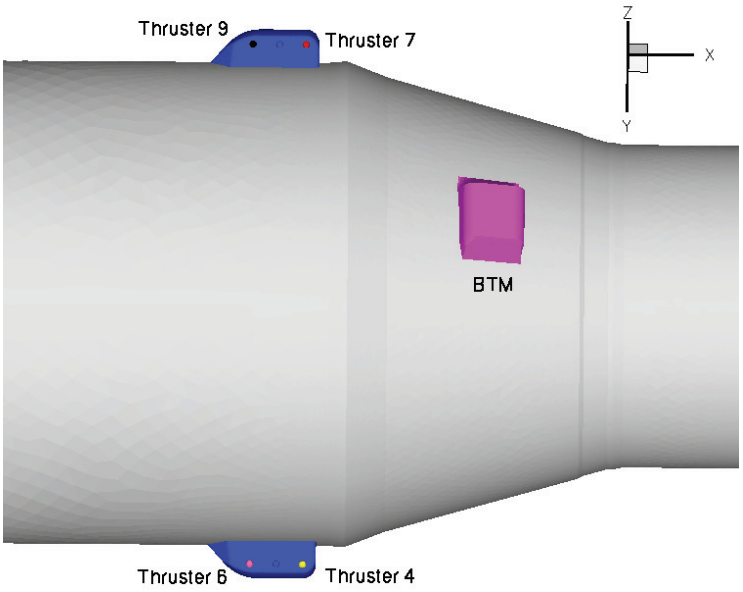

Figure 2: RoCS location.

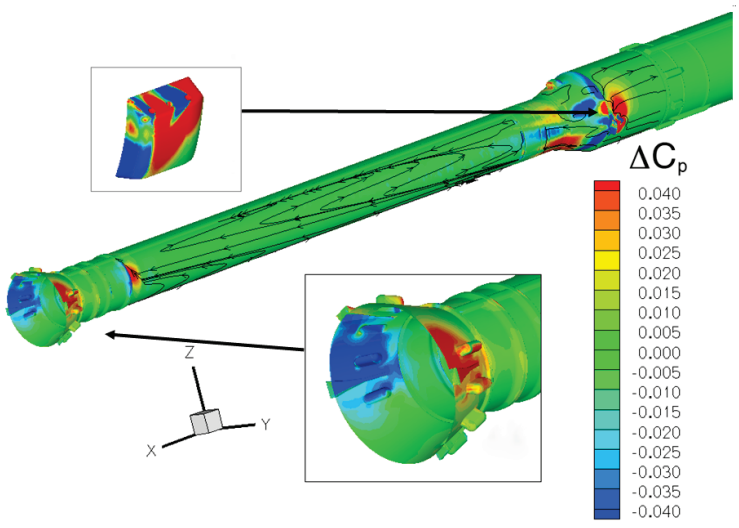

Figure 3: CFD flow contours.

During ascent, the vehicle must remain within 20˚ of the desired orientation, or maintain less than 20˚ roll error. To control the vehicle roll within the allowed tolerance, roll control systems (RoCS) are used. The use of jet control systems is common on missiles and space vehicles. These systems have considerable advantages over conventional surface control. They have shorter response times and are effective at low dynamic pressures. Conventional surfaces may lack control authority, though the flow structure is very complex, and the control efficiency is difficult to predict due to the interaction of the jet with the external cross flow[10–17].

The Ares I RoCS are located near the rear of the interstage, forward of the forward frustrum as shown in Fig. 2. Past jet interaction studies have analyzed jets exiting normal to a body. However, the Ares I control jets exit tangential to the body, thereby attaching and wrapping around the body and impinging on protuberances. Figure 3 shows the jet impingement on the body and protuberances. Areas of warm colors are increased pressure on the body due to the jet interaction with the freestream flow while areas of cool colors represent pressure reductions. The jet interaction effect on the Ares I is very important to quantify. If the impact on the body causes severe reduction or reversal of control authority, a redesign may be necessary.

III. Experiment Methods

This experiment followed the guidelines for designing experiments given by Montgomery[19] and by the AIAA DOE focus group. These guidelines are combined below and are addressed for this research.

Montgomery also presents some points to keep in mind when using statistical techniques in experimentation:

1. Use your non-statistical knowledge of the problem.
2. Keep the design and analysis as simple as possible.
3. Recognize the difference between practical and statistical significance.
4. Experiments are usually iterative.

A. Recognition and Satement of the Problem and Objectives of the Experiment.

The RoCS jet interactions with the freestream air on the Ares I body must be properly characterized to be used in a simulator so that the guidance, navigation, and control engineers can evaluate the control authority of the RoCS system after taking the interactions into account. The characterization should be performed with as much accuracy and efficiency as possible, covering the flight envelope of subsonic through supersonic speeds and all possible angles of attack and roll orientations designated by both nominal and off-nominal trajectories during ascent.

The nature of this experiment is characterization, not exploration or optimization. The experiment is performed using CFD and is known to be non-iterative because of limited CFD server time slot availability. All runs requested must be submitted at one time. For this reason the experiment could not be guided.

The CFD results are deterministic in nature. A deterministic model requires that the DOE experimenter evaluate the necessity of adhering to the three basic principles of DOE and statistical methods. These are replication, randomization, and blocking. Replication is a repetition of the basic experiment and may also be referred to as reproducibility. Replication allows an estimate of experimental error and if the sample mean is used to estimate the effect of a factor, a more precise estimate of that effect can be gained. Randomization is used to force observations and errors to be independently distributed random variables, meaning that each point taken is not affected in any way by any previous data point. This assumption is required when using statistical methods. Randomization is also a good method for averaging out extraneous effects that are not controlled in a test environment but, in time, may affect the responses such as temperature changes. Blocking is used to improve the precision of response estimation between factors that are of no real use to the experimenter but may affect the response values. Blocking can reduce or eliminate variability transmitted by the presence of factors called nuisance factors[19]. For example, Favaregh and Landman[7] reduced the variance in pitch damping of an electrically powered aircraft by blocking the different batteries used. If this experiment were empirically, not computationally based, these principles would have been followed while planning and executing the test matrix. However, because CFD produces no experimental error that can be addressed in this study, there is nothing to be gained in replicating points. Randomization is not necessary because there are no extraneous factors in CFD unless it is designed to produce these effects. Blocking could be performed with CFD if multiple grids and/or multiple individuals performed the analysis and post processing. This however, is out of the scope of this paper and the aero characterization problem itself but could be of interest in future studies. So, deterministic models such as CFD do not need to adhere to the three basic principles.

The major gains in using DOE/RSM for deterministic experiments is the advantage of orthogonal design arrays to minimize the number of data points required for design space characterization and to better characterize the space. Orthogonality is an important property of DOE experiments in that it allows points to be added into a design space to capture effects while retaining uncorrelated factor coefficient estimates. In DOE terms this correlation is called aliasing, and it occurs when the effect of two or more terms cannot be separated into individual contributions.

Any experiment involves risks. These could be making an inferential mistake from the data, such as concluding one design has lower drag compared to another when, in fact, the opposite was true, or characterizing a system output as being linear for a region when in fact it was highly nonlinear. For this experiment there is a risk of poorly characterizing the design space, missing highly nonlinear regions that cause complete loss of control, or control reversal problems in flight past the 20˚ roll error.

B. Relevant Background

Leveraging historical data and expert judgment can greatly benefit estimating the design space and response surface order required for a particular problem. If this information is available, one can decide upon the important factors without using screening experiments commonly used to determine the significant factors. The relevant background available for this data set was two databases developed using CFD and modeling methods during previous Ares I design cycles. The Ares I has had multiple design cycles. When these design changes exhibit significant changes that may affect the aerodynamics, an aerodynamic analysis must be performed. The two previous design configurations, which have been studied for RoCS interactions, are the FTV (also known as the Ares I-X Flight Test Vehicle) and the A103 (previous major configuration to the current one). The A103 and FTV have significantly different RoCS housing designs. This design change affects the jet interaction because of the altered pressure differential on the surface area of the two outer mold line (OML) housings. RoCS housing pressurization contributes

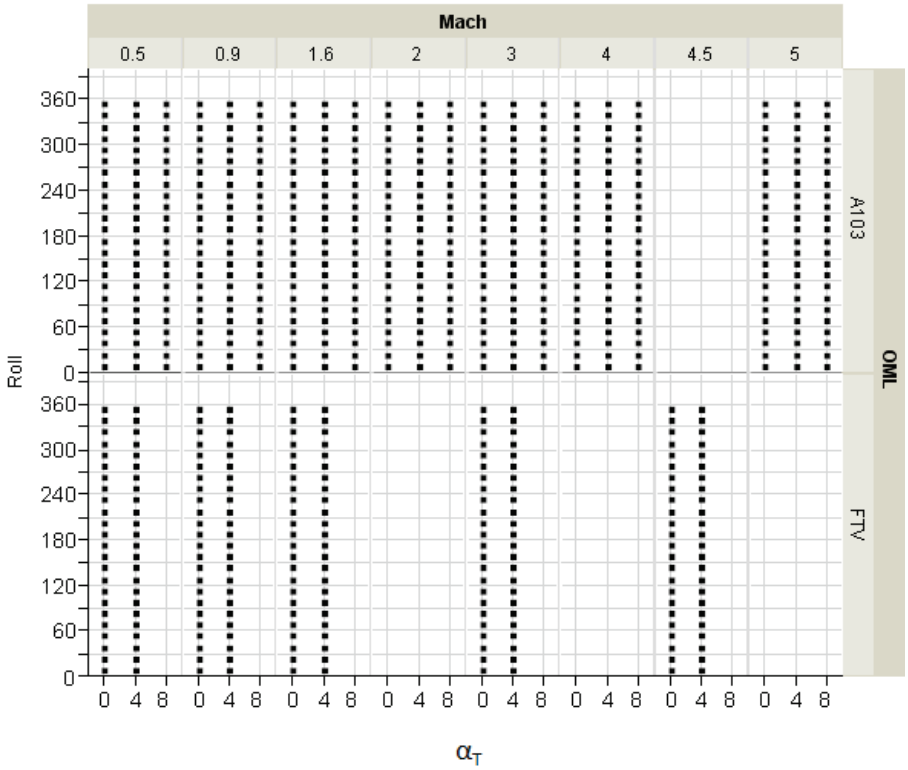

Figure 4: Historical databases.

greatly to the induced rolling moment. The current configuration for this test is the A106. An increase in booster deceleration motors (8 to 10) on the skirt of the first stage and location (mid skirt to aft skirt) was the reasoning for a new analysis for A106.

The previous databases are studied in all factors to determine the necessary experimental design choices to characterize the response of interest adequately. Figure 4 presents the database factor levels. Though the A103 database covers a large area at many levels, the database itself was constructed on limited available CFD, and methods of symmetry were used about a roll orientation angle of 180˚. The FTV database is comprised of CFD estimations for each database value but has only two angle of attack levels. Figure 5 is a typical sample of the datasets. The rolling moment is highly nonlinear across roll angle, nonlinear across the Mach region, and slightly nonlinear across angle of attack.

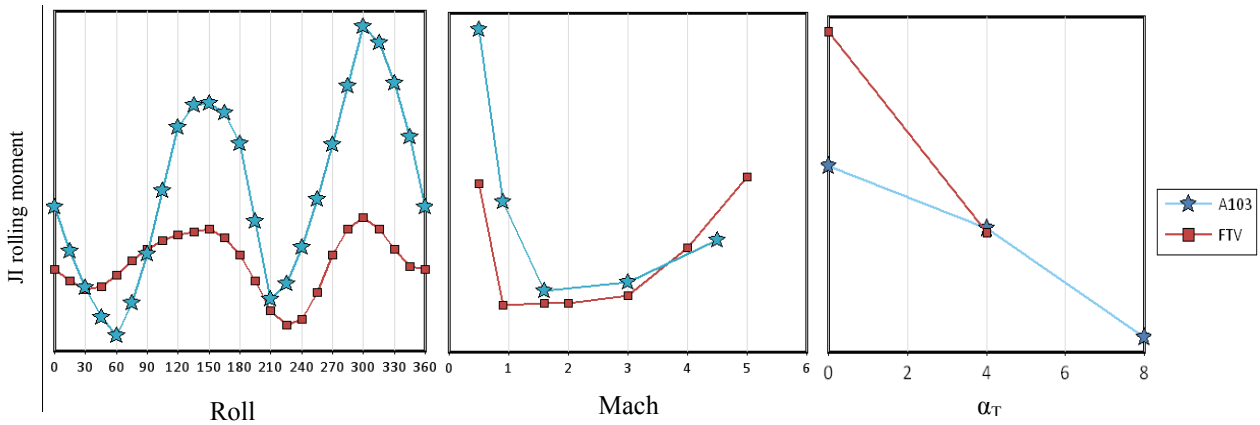

a) Roll variation. **b) Mach variation.** **c) AOA variation.**

Figure 5: Historical jet interaction data.

C. Choice of Factors and Ranges

The factors for this experiment are Mach number, angle of attack, and roll orientation. These factors are consistent for most flight aerodynamic databases for the Ares I. The previous databases and information about the trajectory, such as where the maximum dynamic pressure occurs, was leveraged to select the levels and ranges for

this study. This study contains only Mach 0.5 to 1.6, where previous data showed the most interaction to occur. A constraint is determined by the convergence of the NASA Langley USM3D CFD[20] code, which does not converge for Mach numbers less than Mach 0.78. Therefore, the NASA Ames code OVERFLOW[21] must be used to capture the Mach 0.5 cases.

Table 1: Factors, control variables.

Factor	Units	Range Low	Range High	Priority	Constraints
Mach	N/A	0.5	1.6	1	The CFD code USM3D is not convergent at Mach < 0.78, so the CFD code OVERFLOW must be used for Mach 0.5.
α_T	Degrees	0	8	1	None
φ	Degrees	0	360	1	None

D. Selection of the Response Variable

For the development of this database, there was much discussion about the use of the jet efficiency factor, E_J, versus the jet interaction rolling moment coefficient, $\Delta C_{l,JI}$. Jet interaction literature focuses on the jet efficiency terms in forces and moments[10–17]. The jet interaction rolling moment coefficient is calculated in Eq. (1) and is related to E_J, the jet efficiency for rolling moment in Eq. (2). For ease of implementation into the simulator, the team decided to use the jet interaction rolling moment coefficient, which will be the focus of the analysis.

$$\boldsymbol{\Delta C_{l,JI} = C_{l,RoCS} - C_{l,Freestream}} \tag{1}$$

$$\boldsymbol{E_J = \frac{\Delta C_{l,JI} + C_{l,RoCS,Theoretical}}{C_{l,RocS,Theoretical}}} \tag{2}$$

E. Discussion of Design of Experiments and Response Surface Methodology

DOE/RSM normally relies upon statistical analysis such as analysis of variance (ANOVA) using standard least squares (LS) modeling. This analysis technique has many well understood metrics to provide the experimenter with a clear understanding of the effectiveness of the data and of the extent to which the chosen candidate model captures the information. There are also other types of analysis, such as radial basis function modeling and Kriging interpolation, that can be used to provide effective results.

DOE designs are powerfully efficient because they take advantage of the properties of orthogonal and balanced arrays to estimate the effects and interactions that are necessary or desired to capture the essence of the experiment. The experiments are guided by questions such as "How well do I need to know this information?" or "What exactly am I trying to accomplish with this experiment, and how can I collect the most information in an accurate and efficient manner?" instead of "How many data points can I get with this much money?" Planning an experiment solely on the last question might leave the analyst in a powerless position to improve the product if the goals of the experiment were not met and funds for additional testing are not available. Sequential analysis and building of the experiment is important to ensure all the goals are met during the experiment, not afterwards. Unfortunately for most, sequential testing is unavailable, as was the case here. The entire design was required up front with no opportunity for in-situ analysis.

Each point where data is taken is referred to as an observation. This observation occurs, most likely, at set variable levels. These variables are called regressors, and they are normally the variables assumed to cause a significant change in the response. The response is the system output at the regressor levels. This response is commonly analyzed using least squares methods.

Standard Least Squares. For standard least squares (LS), let n be the number of observations, in this case CFD points, and let k be the number of regressors (terms in the model). Assume a response variable y (rolling moment) with $n > k$ observations. Each regressor variable will have a value x_{ij} at the i^{th} observation and j^{th} level. The general model equation in terms of observations is[22]

$$\boldsymbol{y_i = \beta_0 + \beta_1 x_{i1} + \beta_2 x_{i2} + \cdots + \beta_k x_{k1}} \tag{3}$$

$$= \beta_0 + \sum_{j=1}^{k} \beta_j x_{ij} + \varepsilon_i$$

$$i = 1,2, \ldots, n$$

The error terms ε_i are assumed to have a mean E(ε) = 0, have a variance σ^2, and be uncorrelated random variables. The method of LS is to solve for regression coefficients, βs, while minimizing the error. To accomplish this, the error term is solved for in terms of y and βs and this function is then minimized.

$$\boldsymbol{L = \sum_{i=1}^{n} \varepsilon_i^2} \tag{4}$$

$$= \sum_{i=1}^{n} (y_i - \beta_0 - \sum_{i=1}^{n} \beta_j x_{ij})^2$$

Here are the equations in matrix form, appropriate for a series of data.

$$\boldsymbol{y = X\beta + \varepsilon} \tag{5}$$

$$y = \begin{bmatrix} y_1 \\ y_2 \\ \vdots \\ y_n \end{bmatrix}, X = \begin{bmatrix} 1 & x_{11} & x_{21} & \ldots & x_{1k} \\ 1 & x_{12} & x_{22} & \ldots & x_{1k} \\ 1 & \vdots & \vdots & \ddots & \vdots \\ 1 & x_{n1} & x_{n2} & \cdots & x_{nk} \end{bmatrix}$$

$$\beta = \begin{bmatrix} \beta_1 \\ \beta_2 \\ \vdots \\ \beta_k \end{bmatrix}, \varepsilon = \begin{bmatrix} \varepsilon_1 \\ \varepsilon_2 \\ \vdots \\ \varepsilon_k \end{bmatrix}$$

To find the minimum point of error, the partial derivative of function L is taken with respect to β and set equal to zero.

$$\left.\frac{\partial L}{\partial \beta}\right|_b = -2X^T y + 2X^T X b = 0 \tag{6}$$

$$X^T X b = X^T y$$

$$b = (X^T X)^{-1} X^T y \tag{7}$$

$$\hat{y} = Xb \tag{8}$$

The solution of b is now the LS estimator of β and $\hat{y}$ is the estimation of y. For this case, the team is not particularly interested in the values of b, as would be the case if trying to estimate static and dynamic derivatives of aircraft or rocket equations of motion. In this case the team is only interested in a good fitting model that comes reasonably close to the observations ($\hat{y}$ close to y), has good prediction, and has a minimum of poor characteristics such high variance inflation factors or low adjusted and predicted goodness of fit values (these will be explained further in this section).

Weighted Least Squares. For normally distributed errors, standard LS produce estimators with good statistical properties. For non-normal distributions, those with longer or heavy tails, outliers in these tails may have a strong influence on the LS estimate, pulling the fit too much in the outlier direction.

A single weighted LS estimation is a simple adjustment to standard LS but allows the experimenter to use additional knowledge of the data to produce a more robust and accurate model. Weighting is a process that explicitly defines the goodness of a point. For example, a time averaged observation may give differing error at different

factor levels, such as high α_T versus low α_T. If the high α_T responses have a higher error, they should be assumed not to be as good as the low α_T points and therefore, should be penalized.

Each observation y_i may have a measurement error associated with it, w_i. This error may then be used as a weighting parameter. The experimenter shoud create a diagonal matrix of the weights.

$$W = \begin{bmatrix} w_{11} & 0 & 0 & 0 \\ 0 & w_{22} & 0 & 0 \\ 0 & 0 & \ddots & 0 \\ 0 & 0 & 0 & w_{ii} \end{bmatrix}$$

To obtain the LS estimator b, apply the weighting matrix to the least squares normal equations and estimate $\hat{y}$ accordingly with Eq. (8).

$$b = (X^T W X)^{-1} X^T W y \tag{9}$$

Useful Metrics. Statistical metrics help the analyst determine the effectiveness of the data and the adequacy of the regression models used. They can help determine the adequacy of the design itself and guide the experimenter in augmenting the design to guard against any undesired inadequacies, such as poor prediction. There are many metrics that the analyst may choose to guide the experiment and analysis. Some may never use any metrics, relying solely on visual inspection. In this analysis the prominent metrics used are variance inflation factors, predicted scaled variation, and goodness of fit.

Variance inflation factors (VIFs) check for multicollinearity among the regressors. Multicollinearity is defined as near linear dependence among regressors that can have serious effects on model parameter estimates and the applicability of the model. If multicollinearity is present, the variance and covariance of the regressors can possibly become large[22], depending on the level of multicollinearity. In the case that VIF values are equal to 1, the design is completely orthogonal and no multicollinearity exists. In general, VIF's should be less than 10 to indicate that multicollinearity is not a serious problem. In the case that the VIF is very high, one can take additional data aimed specifically at breaking the multicollinearity, though this may not be possible if discovered post test. Another method to reduce multicollinearity is to reduce the number of terms in the model. High multicollinearity does not necessarily translate into an inadequate model, but the individual regressor coefficients that have high VIFs will be poorly estimated. The model itself may be estimated well. It is important to check the design for multicollinearity if the goal of the experiment is to estimate the regression coefficient values. It is also important to visually inspect the model for over-fitting due to retaining regressors with high VIFs, which can lead to poor internal estimation and very poor extrapolation. For this analysis, low VIFs are certainly preferred, but overall good model fitting is a higher priority.

The metric prediction variance and the property of rotatability provide measures of stability (reasonably stable distribution of the prediction variance[22]) throughout the design space. Prediction variance gives an estimation of the predictive capability of a single point at a distance from the design origin. Rotatability is a property that indicates that the prediction variance of two locations in the design space that are equidistant from the design center should be equivalent. These two metrics rely solely on the design of the experiment and not at all on the actual responses.

Goodness of fit metrics are well known and understood. These metrics are reasonable to use for comparing candidate models. The widely used R^2 value is a measure of the variability captured by the chosen regression model. However, using standard LS analysis, adding regression terms to the model artificially raises the R^2 value as the calculation is solely dependent on the sum of squares of the regression model and the total sum of squares. The more terms present in the model, the higher the regression sum of squares, giving no consideration of statistical significance. The adjusted R^2 value normalizes the goodness of fit by the number of terms in the model. So, if adding non-significant terms decreases the adjusted R^2 value, they should not be included. If the adjusted R^2 value becomes very low compared to the R^2, the model is over defined, and either more points should be added or a lower order model should be used. The predicted R^2 value gives a good indication of the prediction of the model. The prediction error sum of squares (PRESS) is the determining factor in the predicted R^2 value. Lower PRESS is better. The PRESS estimates the model stability in the case that each observation was individually removed and a new model was fitted omitting that observation. The difference between the removed observation and the model gives a metric of prediction and individual observation leverage. If an observation has such high leverage that it dramatically influences the model, it should be investigated for validity. Replicates or an additional local inference space should be used to alleviate the high leverage, if possible.

F. Choice of DOE Experimental Design

The present experimental design is a DOE full factorial (vertex points) augmented with axial points, constraint plane center points, and a mean overall center point, resulting in 23 cases for each sector, shown in Fig. 6. The full factorial estimates the main effects and two factor interactions. The constraint plane center and overall centers estimate the mean and add degrees of freedom to estimate quadratic terms. The axial points estimate quadratic terms. The levels were chosen so that all the points fell on cardinal Mach, roll, and α_T values. The experiment design is repeated every 60˚ of roll, which are referred to as individual sectors. This design is capable of capturing up to a full quadratic model with interactions as shown in the Taylor Series expansion of Eq. (10) in each sector. Sectors 1 and 2 share the points at 60˚ while sectors 2 and 3 share points at 120˚, and so on (Fig. 7).

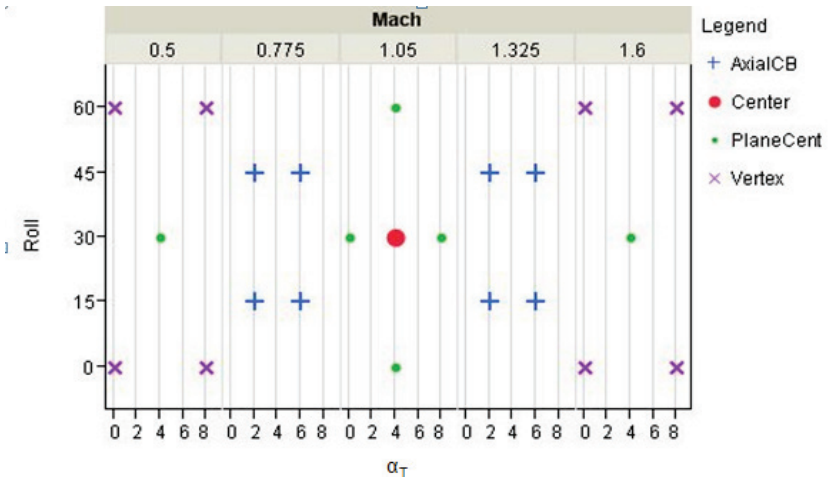

Figure 6: First sector factor levels.

Figure 8 presents the design space as a cube with the design points inside the cube. An important quality about this design is that it is bounding so that no extrapolation is necessary within the range of all factors. The total number of points to capture the nonlinear model using this design is 108 compared to 196 if a cardinal grid were used to capture similar effects.

$$Y = \beta_0 + \beta_M M + \beta_\alpha \alpha + \beta_\varphi \varphi + \beta_{M\alpha} M\alpha + \beta_{M\varphi} M\varphi + \beta_{\alpha\varphi} \alpha\varphi + \beta_{M_2} M^2 + \beta_{\alpha_2} \alpha^2 + \beta_{\varphi_2} \varphi^2 \quad (10)$$

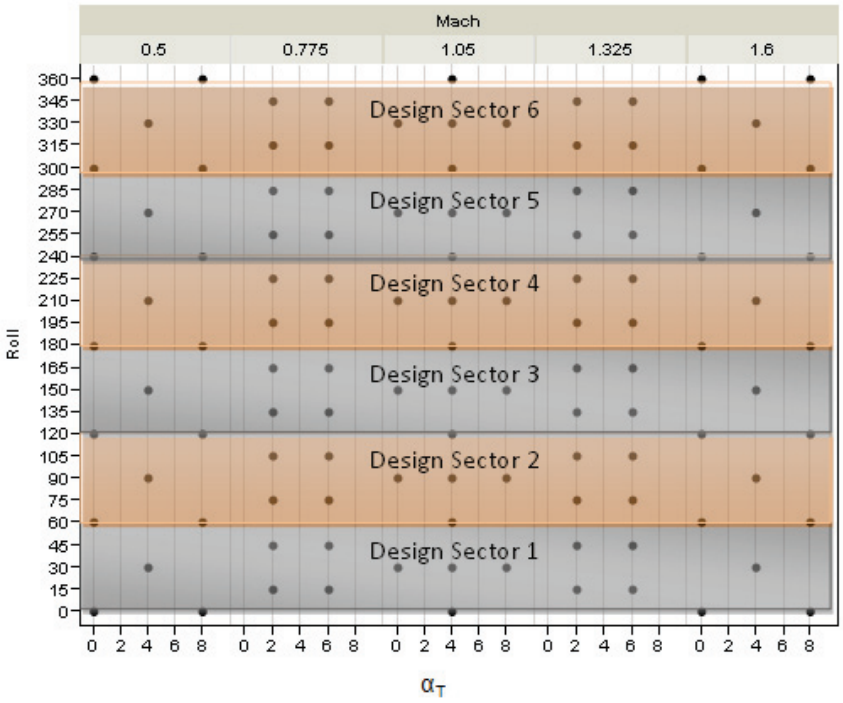

Figure 7: Design space with all sectors.

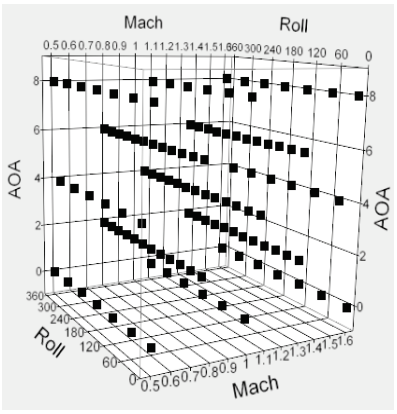

Figure 8: Three dimensional view of the design space.

As mentioned in the discussion of metrics, this experiment should be analyzed for prediction stability and rotatability. Rotatability is retained well within individual sectors and across all sectors as shown in Fig. 9 and 10. A perfect model of rotatability is one with concentric circular contours. Concentric rectangles or near circular models are certainly adequate. Scaled prediction variance plots with completely misshapen contours, or those not centered about the origin, would not have the property of rotatability. Figure 9 shows the scaled prediction variance of the first sector, is applicable to each individual sector, and is based on the candidate model of Eq. (10). Figure 10 shows the full design space with the design points across all sectors. Although Fig. 10 shows some variation along the prediction variance contours, the general form of the contours shows reasonable stability. These prediction variance values are based on assuming a 6th order model in roll, 2nd order model for Mach, and α_T.

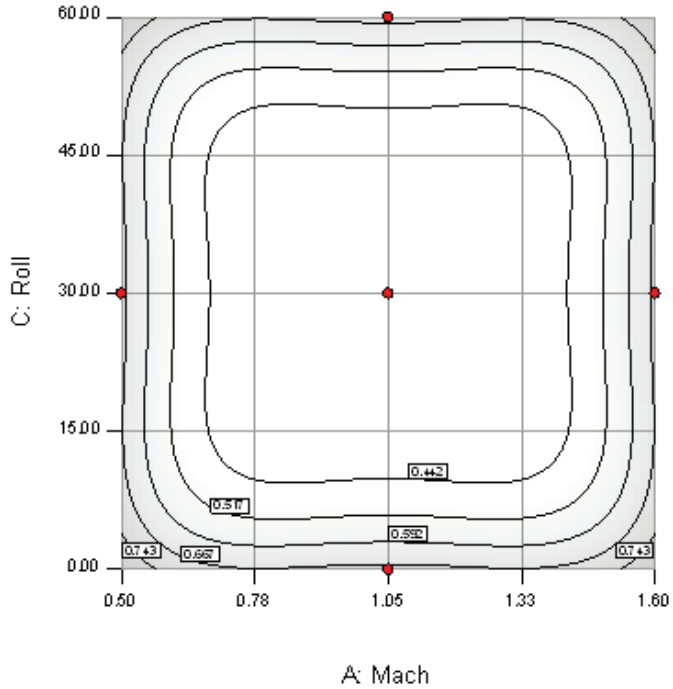

Figure 9: Scaled prediction variance of single sector at α_T = 4˚.

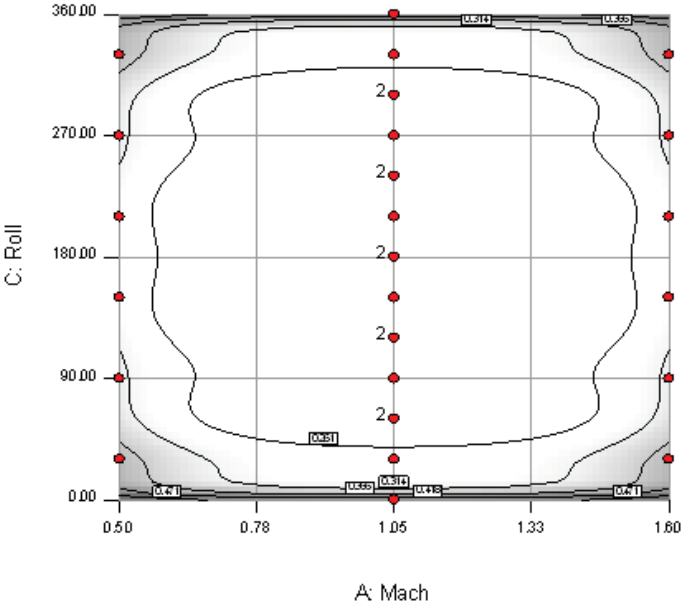

Figure 10: Scaled prediction variance of entire design space at α_T = 4˚.

G. Performing the Experiment

CFD modeling was used for the entire experiment. There is no CFD validation data for this particular application so the uncertainty is not known. Two CFD codes were used for the analysis. USM3D CFD analysis was performed at NASA Langley Research Center for Mach values of 0.78 to 4.5. Overflow CFD, performed at NASA AMES Research Laboratory, provided data for Mach 0.5. The external flow conditions were obtained from available trajectory information and relied solely on Mach, not on α_T or roll angles. Table 2 shows the flow conditions. The jet exhaust is modeled as a perfect gas (γ = 1.4). A RoCS firing-on case and a RoCS firing-off case were performed at each candidate point in the design space. Because of some communication mishaps across teams, not every case was performed at the exact factor levels as requested, but these were few and did not significantly affect the outcome of the modeling, in most cases. The next section discusses more on the effect of missing cases.

It was assumed that data obtained at an α_T = 0˚ could be applied to all roll angles at that angle, i.e., data at α_T = 0˚; φ = 0˚ is equivalent to every data point at α_T = 0˚; φ = 0˚ to 360˚. These points are not held constant in the response surface plots, though the final product would contain this feature.

Table 2: External flow conditions.

Mach	T (R)	Re/ft	P_{ATM} (lb/ft^2)	ρ(lb/ft^3)
0.50	514	290,0000	1716	0.001935
0.80	491	3,600,000	1265	0.001500
0.90	480	3.700,000	1113	0.001350
1.05	462	3.700,000	907	0.001144
1.20	442	3.700,000	738	0.000973
2.00	371	2,900,000	277	0.000437
3.00	386	1,200,000	80	0.000122
4.00	414	430,000	25	0.000034

IV. Analysis Methods

A. Analysis of the Data

Four types of analysis were performed for evaluation. First, an analysis fitting one high order polynomial to the entire data set was performed. Second, quadratic models were fitted to individual sectors, and the estimated responses were averaged where the surfaces join. Third, a quadratic model was fit in 60˚ roll sectors every 15˚, creating constantly overlapping response surfaces that can be averaged in the entire design space. Fourth, overlapping sectors from the third analysis were used along with recursive weighting techniques to minimize the maximum roll coefficient derivative when retaining CFD values.

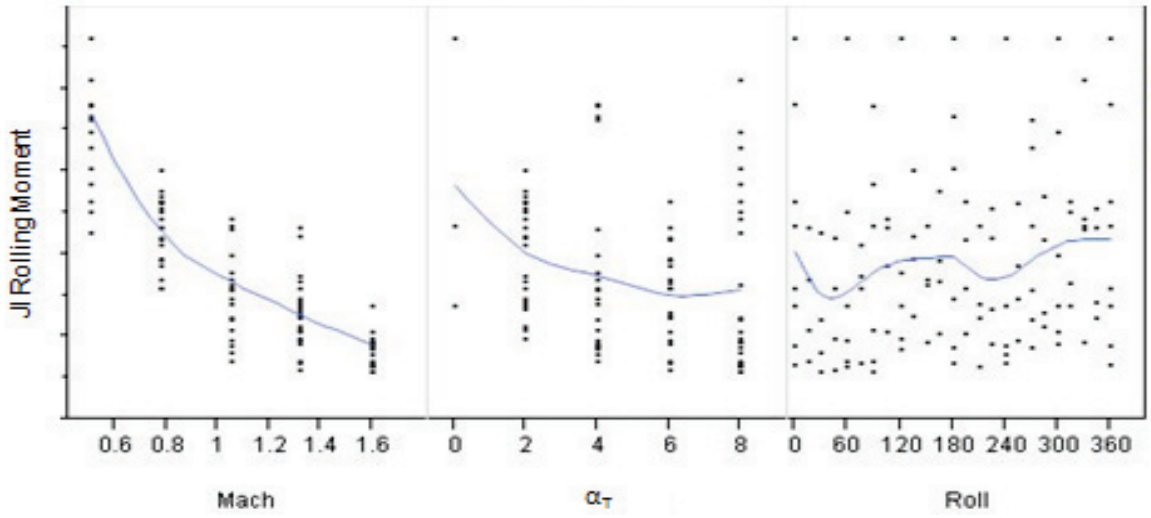

Figure 11: Jet interaction rolling moment vs all factors.

Plotting the response versus all factors before fitting the model can give the analyst an idea of the main effects before getting into the analysis. Figure 11 contains three subplots that contain all the response values in each plot with an averaging line between groups of points. Clearly the response generally decreases as Mach increases. A correlation of Mach and the difference in total pressure and jet exit pressure may exist, but was not considered in this analysis. The response shows a decrease with α_T but not as strong as the Mach effect. The response in roll shows no trend, indicating either no dependence or highly nonlinear behavior that is dependent on interactions with the other factors. The maximum value across roll is the repeated $\alpha_T = 0^\circ$, $\varphi = 0^\circ$ case.

In the following sections a response surface of the estimated model and a response surface with CFD are plotted. When plotting the estimated model alone, the response is of the general form $\hat{y} = Xb$, herein referred to as Model A. When including the design points, the response is of the general form $\hat{y} = Xb + \varepsilon$, herein referred to as Model B. The distinction highlights an important discussion for deterministic experiment model analysis. Should the absolute values remain in the model or should the general trends of the model stand alone? A pro for adding the residual, ε, back to the model is that at those points in the model, the estimation is exact, and since there is no replication for

deterministic models, there should not exist another value for that locale. However, the prediction of new points near that locale will not necessarily be made better by including those points. In fact, the newly predicted points may be worse if the residual has a high leverage on the model. The confidence intervals of the model will also be affected. If the model includes the residuals, then no residuals exist for a residual analysis, therefore the only means of obtaining error is to take validation points. While taking validation points is always a good idea to be sure the model is predicting well in the design space, it should not be the only means of evaluating prediction error. It is the author's opinion that if the model can be made smooth with the addition of the residuals to the model, that model B should be used and the error from the model A should be applied to model B.

B. Single Regression Model Analysis

The single regression model has degrees of freedom (DOF) available for 2nd order Mach and angle of attack terms and enough DOF for a 12th order roll term. The goodness of fit is optimal, however, at the 5th order roll term.

The model structure for this analysis is:

$$\Delta C_{l,JI} = \beta_0 + \beta_M M + \beta_\alpha \alpha + \beta_\varphi \varphi + \beta_{M\alpha} M\alpha + \beta_{M\varphi} M\varphi + \beta_{\alpha\varphi} \alpha\varphi + \beta_{M_2} M^2 + \beta_{\alpha_2} \alpha^2 + \beta_{\varphi_2} \varphi^2 + \beta_{\varphi_3} \varphi^3 + \beta_{\varphi_4} \varphi^4 + \beta_{\varphi_5} \varphi^5 \quad (11)$$

Overall the model performs very well. Figure 12 presents the single regression model at $\alpha_T = 4^\circ$. The model performs worst at a Mach number of 1.32 and $\alpha_T = 2^\circ$. In this region, the data has high amplitude that is not captured well by this global model. Figure 13 includes the design points into the response at Mach 1.32 and clearly shows how the CFD, when added back in, largely pulls away from the surface, as well as creates large derivative changes where there exist two CFD points and one regression model point between them. This indicates that there is still something to be gained over the single regression model. The model is hierarchal, i.e., it includes all terms of lower order. The model goodness of fit (R^2) values are $R^2 = 0.9488$, adjusted $R^2 = 0.9431$, and predicted $R^2 = 0.9348$. All goodness of fit values indicate that most of the variance in the data is captured by the model. The R^2 is reasonably high, though a higher value is always desirable. The adjusted R^2 is well in line with the R^2, indicating that the model is not being over-fitted to capture the data well and that 94.31% of the variability in the data is captured by the model, leaving almost 6% to fitting error. A predicted R^2 value within 2% of the R^2 suggests very good robustness in the model and insensitivity to missing data or highly leveraged points. The VIFs are very high (>10) for higher order roll terms. In order to reduce them below a value of 10, the model can be reduced to 3rd order, though when reduced, the model does not capture the desired trends in roll. This is an attribute of the highly nonlinear nature of the aerodynamic system.

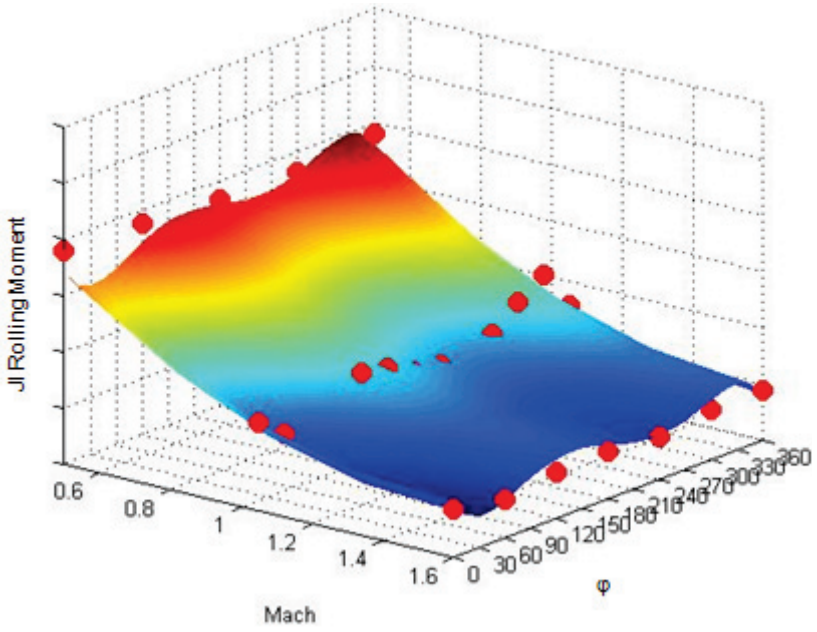

Figure 12: Single regression model.

C. Multiple Sector Regression Analysis

The initial plan of the experiment design was to capture up to 2nd order behavior every 60° of roll. For the multiple sector analysis, backward elimination least squares (LS) regression was used to develop analytical models for each sector. Each sector is estimated initially by the model in Eq. (10) and insignificant terms removed. This method produced a combination of reduced and full models, depending on the significant variables in the sector spaces. Figure 14 shows the goodness of fit values.

The majority of R^2, adjusted R^2, and predicted R^2 values seems very reasonable and indicates adequate modeling of the variance in the

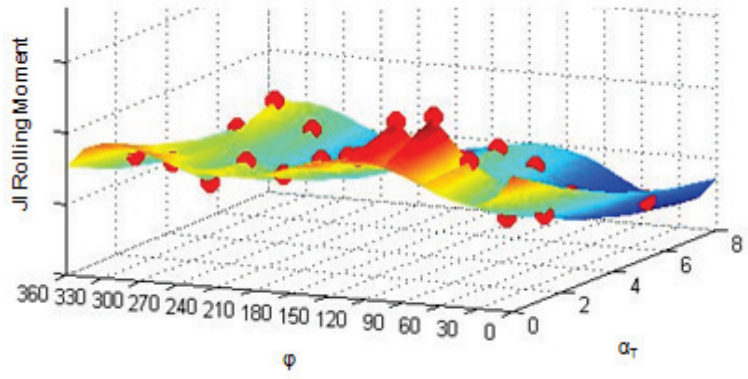

Figure 13: Single regression model including design points.

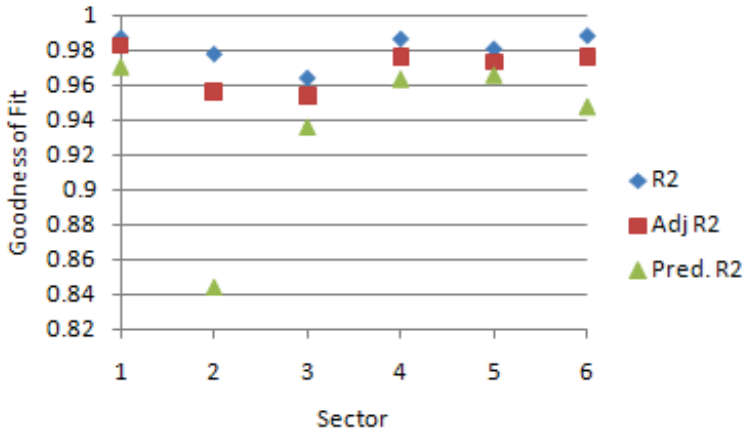

Figure 14: Goodness of fit metrics for multiple sectors.

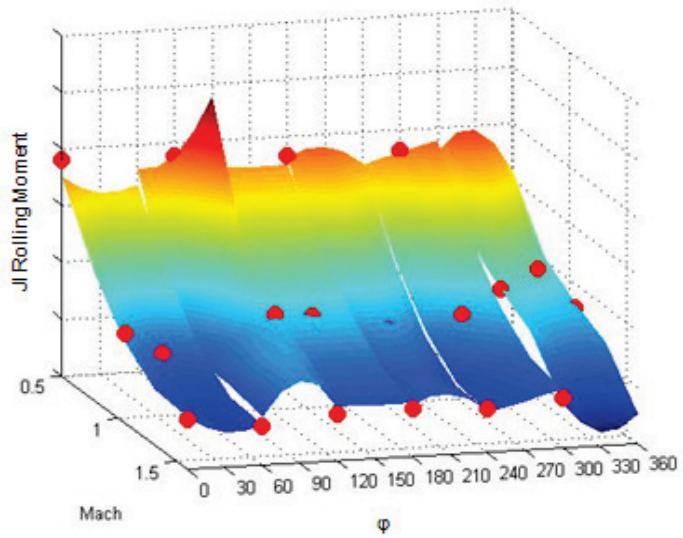

Figure 15: Multiple sector response surfaces.

data. The exception is sector 2, which has a significantly low predicted R^2 value. Figure 15 shows the multiple response surfaces with the corresponding CFD points (not included in the model) at $\alpha_T = 4^\circ$. Each sector modeled the data well, individually, with the exception of the 60° to 120° sector (sector 2). Unfortunately, sector 2 is missing a data point at Mach 0.5, $\alpha_T = 8^\circ$, $\varphi = 120^\circ$. The sector was not bounded as was designed, extrapolation was necessary, and, therefore, an extremely poor prediction ensued, as shown by the low predicted R^2 values and visual inspection of the response surface with the corresponding data.

The high sensitivity of this approach to missing data is highlighted with the red tipped spike at 120° roll. This poorly predicting response is not present in the single regression model analysis. Significant differences also exist in response models where they join. These differences will cause a final averaging of the sectors to contain undesirably high derivative changes across roll. The averaged R^2 value for the global model = 0.9811, adjusted R^2 = 0.9698, and predicted R^2 = 0.9381. The VIFs were very low for most sectors, indicating a near orthogonal design for the chosen modeling as was planned, again with the exception of sector two, which had some collinearity because of the missing data.

While this analysis was the planned choice for modeling the data, and the overall goodness of fit values show a better fit than the single response surface analysis, the consequences of this modeling are unacceptable. The author then attempted another type of modeling to alleviate the pitfalls of this one by applying an extension of the multiple sector analysis.

D. Continuous Sector Regression Analysis

The aim of continuous sector regression analysis is to create a globally robust model, insensitive to missing data, and highly locally accurate in regions where the single regression model was inadequate. The models are built in 60˚ roll spaces, overlapping by 15˚. The model used is the same as Eq. (10).This scheme allows each point in the design space to be estimated by four response surfaces. Each estimate is then averaged to create an averaged global surface. Advantage is taken in the circular referencing of roll; i.e., 15˚ = 375˚ and 30˚ = 390˚ etc. This property ensures all points are covered by four response surfaces.

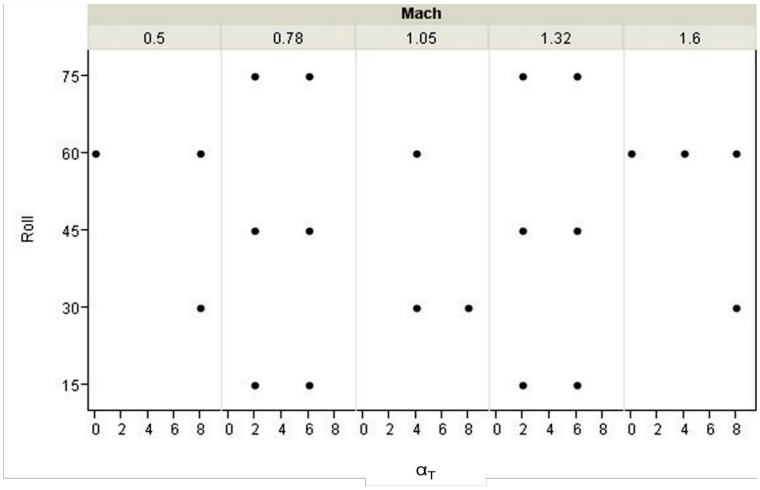

Figure 16: First offset sector available data points (not pure design points).

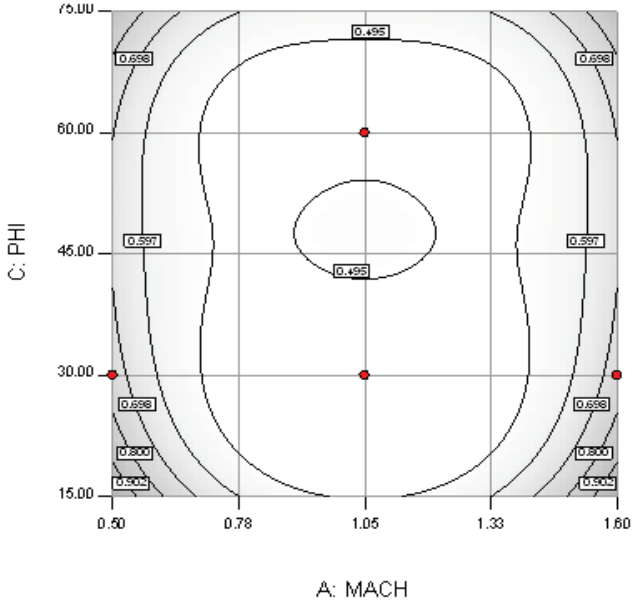

Figure 17: Scaled predicted variance for the first offset sector.

Before using the original test matrix in an unplanned fashion, the matrix must be tested for adequate properties in these in-between sectors. Figure 16 represents the available data in the first offset sector from roll values of 15˚ to 75˚. Figure 17 shows that the data is very near rotatable, a desired attribute. The VIF are very low for a 2nd order model within this design space. It is feasible then to fit a 2nd order model to this data in each offset sector. A downside to the offset sector design space is that the model is extrapolating for values of Mach 0.5 and 1.6 at roll angles of 15˚ and 75˚. Fortunately, there are four estimations at each point, with only one as an extrapolated value, so the extrapolation effect is minimal.

Figure 18 shows the continuous sector response surface. From both visual inspection and model quality metrics, the model seems to perform well. When retaining the CFD values in the response surface, it blends smoothly, with the exception, again, at Mach 1.32, α_T = 2, though in this region it does perform better than the single regression model. The overall goodness of fit values are R^2 = 0.965, adjusted R^2 = 0.960, and the predicted R^2 = 0.964. A predicted R^2 value that is almost identical to the R^2 value is a clear sign of robustness in the modeling, meaning that even though data was not available for some cases, it has a negligible effect on the resulting model, unlike the multiple sector analysis.

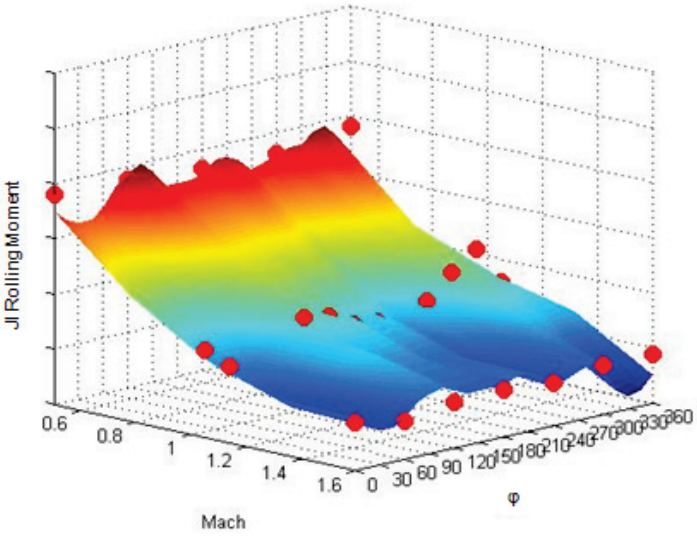

a) Without design points.

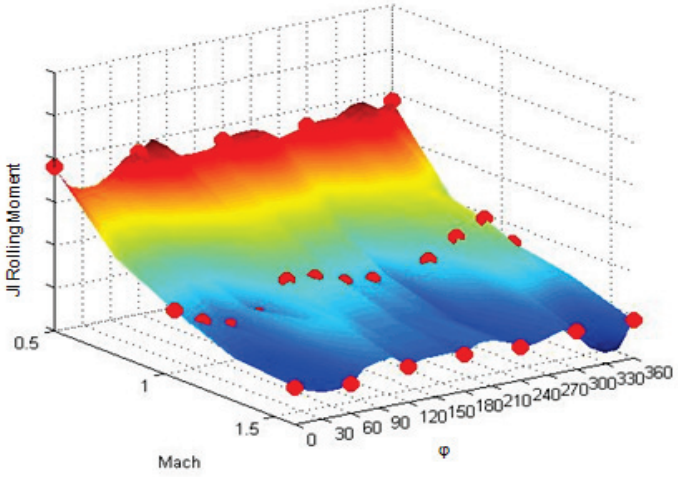

b) With design points.

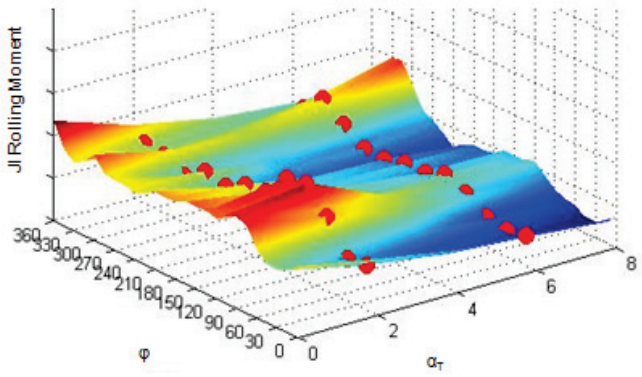

c) With design points at Mach 1.32.

Figure 18: Continuous sectors.

E. Recursive Weighted Sector Regression Analysis

The goal of performing recursive weighted sector regression (RWSR) analysis is to increase the accuracy and smoothness of local regression models. This is attempted by first obtaining a global model, then using estimations from the global response surface as down weighted system response points, while using the true CFD observations as highly weighted values. The global model could be that from the single regression model or from the continuous sector model because each has similarly good properties. The weighted LS Eq. (9) was used to calculate new LS estimators and $\hat{y} = Xb + \varepsilon$ obtained the new model estimate. A code was developed to perform this iteration on mini-sectors using roll increments of only 5° and performing the RWSR on 30° wide sectors (in roll). The CFD and response surface estimations were weighted using the variance associated with the CFD response. This creates an equal weighting that must then be varied using a weighting ratio, shown in Eq. (12), where *w* is the diagonal weight matrix. The reason for showing the denominator in this equation, even though it has no effect in this case, is that it creates a placeholder for using differing weighting denominators, such as those that can be used if wind tunnel and CFD results were combined. The CFD weight is varied to understand the effect of different weighting ratios (*WR*).

$$w(ii) = \begin{cases} \frac{1}{var(y)}, & if\ RS \\ \frac{WR}{var(y)}, & if\ CFD \end{cases} \tag{12}$$

The maximum response roll derivative was tracked until a minimum was reached to ensure smoothness in roll, shown in Fig. 19. Examining the *WR* in the response surface metrics gave an insight into what weighting can do to a surface. The higher the weight given to the CFD, the more the surface is pulled to those points. This has a direct effect on the residuals of the true data to the surface. The higher the *WR* values, the lower the residuals. Also, as the *WR* is increased, the maximum jet interaction (JI) rolling moment derivative with respect to roll was minimized exponentially faster, and the value of the derivative was lower for higher *WR*.

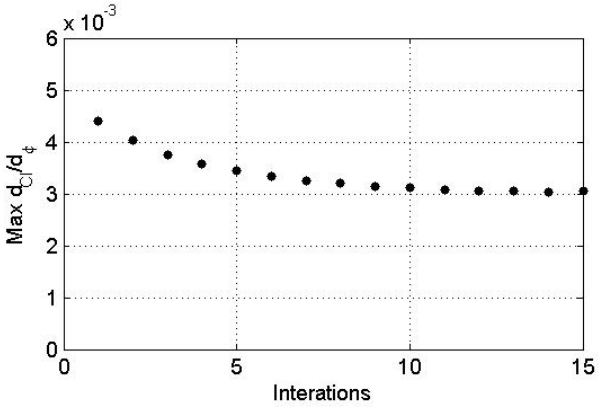

Figure 19: Maximum JI rolling moment derivative with respect to roll when including the design points.

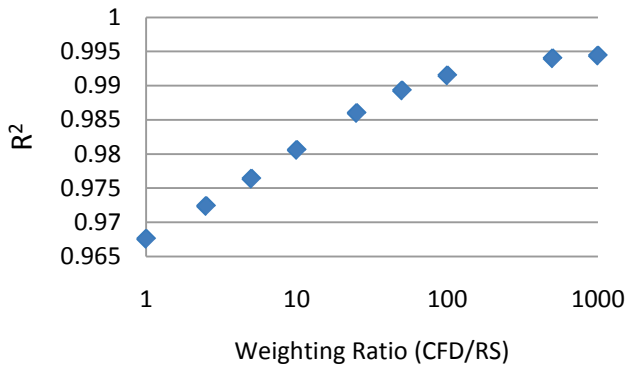

Figure 20: Influence of weighting ratios.

The drawback of high *WR* is the considerably high flexibility in the model. This high flexibility must be restrained to reasonable levels to not induce too much variation in the model in order to reach the outer lying points. The influence of the *WR* on goodness of fit is shown on a log scale in Fig. 20.

The R^2 values increase logarithmically, implicitly depicting the decrease in residuals. So the art is to select the *WR* to allow smooth transition to true CFD points without inducing undesired variability and retaining a low maximum derivative. In this case a value of 10 was chosen that reduced the maximum derivative 30% (Fig. 19).

The overall goodness of fit values are R^2 = 0.9806, adjusted R^2 = 0.9782, and the predicted R^2 = 0.9804. Although the goodness of fit value gain seems to be very marginal over that of the previous methods, the availability to include the deterministic points appropriately makes this approach the most robust (it is least influenced by missing data) and most accurate (it captures the known data well while not inducing unreasonable variation in the model). This approach is also simple to program and implement. Figure 21 presents the final model with *WR* = 10 at Mach 1.05.

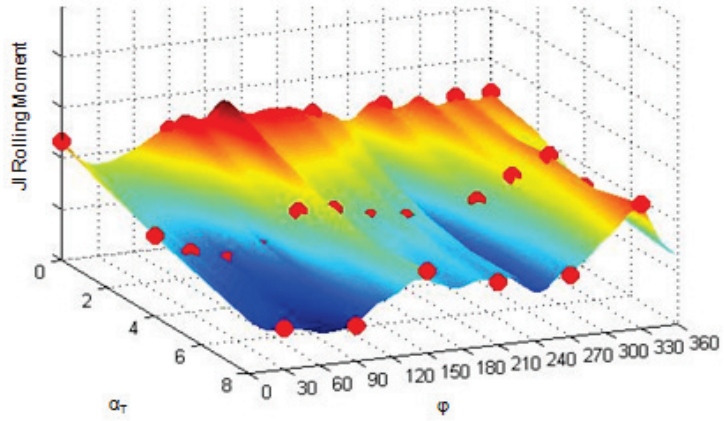

Figure 21: RWSR model at Mach 1.05 including design points.

Montgomery[22] presents an optimization technique called *iteratively reweighted least squares* that can be applied to this problem of including deterministic data into a surface smoothly as well as blending deterministic and experimental results. The application of this method is worthwhile for future work and is briefly introduced.

While the name sounds similar to the recursive weighting method just discussed, the weighting is different. To perform iteratively reweighted least squares, an initial estimation of b is obtained, indexed as b_0. The weighting is then a diagonal matrix with elements w_{i0} such that

$$w_{i0} = \begin{cases} \psi[(y_i - x_i' b_0)/s], & if\ y_i \neq x_i' b_0 \\ 1, & if\ y_i = x_i' b_0 \end{cases} \quad \text{(Ref. 22)} \tag{13}$$

$$\boldsymbol{b_m} = (\boldsymbol{X^T W_m X})^{-1} \boldsymbol{X^T W_m y} \tag{14}$$

where s is a robust estimate of the standard deviation, i is the observation, m is the iteration index, and ψ is an influence function that controls the individual weights of residuals, applicable within a range of tuning factors. The function of residuals, which is to be minimized, is called a robust criterion function. Montgomery[22] gives a handful of commonly used robust criterion functions with corresponding influence functions and weights. Eq. (9) is modified to provide iterative coefficient estimations.

F. Validation

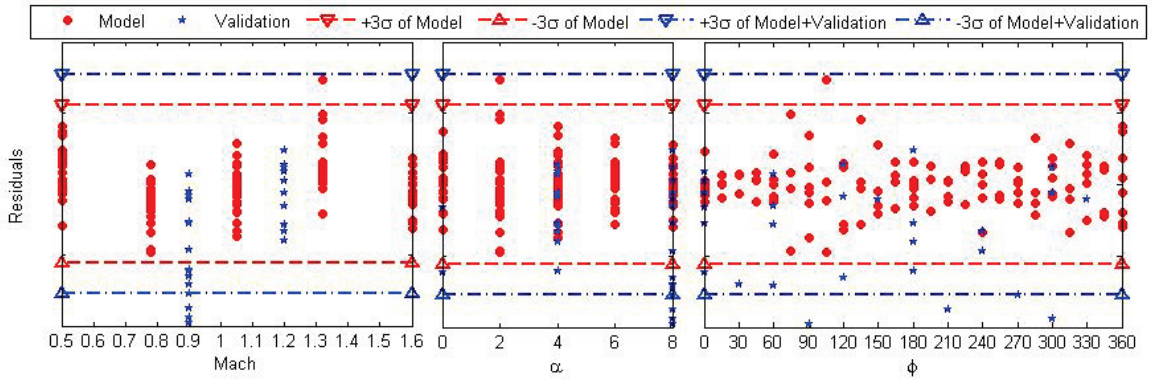

Figure 22: Residuals to model error and validation.

No model should be relied upon without having estimated error predicting points inside the area of operation. Validation points were used to evaluate the predictability of the model at off-design points within the area of operation of this response surface. In a wind tunnel test setting, these points would be used to exercise the model and guide the experiment into regions if the prediction is not within tolerance. For this CFD study, validation directly aids the development of an uncertainty model for the response surface. The RWSR model was used to predict the response at 28 available validation points[†]. These points were not used in the creation of the response surface. The validation points were at Mach 0.9 and 1.2. Residuals of the RWSR predictions and the validation residuals are plotted in Fig. 22. A three standard deviation dispersion bound is plotted for the model-only residuals and for the

[†] Even with the additional 28 validation points, the total for this experiment is 60 fewer points than for the cardinal grid. Each case consists of a power on and power off case, so the real savings is 120 CFD runs.

model + validation residuals. While these bounds do not represent the actual bounds that would be chosen given this data set, they do show the general fitness of using bounds created without validation points compared to bounds created with them. Mach 0.9 validation points show deviation from the model, which is not surprising given the flow physics associated with transonic flow near Mach 1. An inspection of the residuals versus Mach indicates an uncaptured 3rd order Mach variation. The model could be refitted including the validation points with a $\beta_{M_3} M^3$ term to create a more constant variation across Mach. The residuals are mostly constant across α_T, but there is certainly more variation in the second sector of roll, 60 to 120°, than in the rest of the sectors. If experiment iteration were possible, an augmentation to the design in this sector would have added the additional DOF to capture the large variations in roll. Having constant error across all factors is preferred. It means that the model is going through the mean of the data at all levels and that all variance from factors is captured. If the error is constant, the uncertainty becomes a simple value that can be applied across the entire space.

Figure 23 shows the modeling residuals when including the available validation points in the modeling. These plots show a constant variance across all variables; no longer are the residuals varying with Mach and roll. There is a significant improvement over the model constructed without the validation cases. Had sequential testing been performed, these cases would have proven very valuable to guiding the test. Luckily, having the foresight to check at these conditions turned out to be a sound decision.

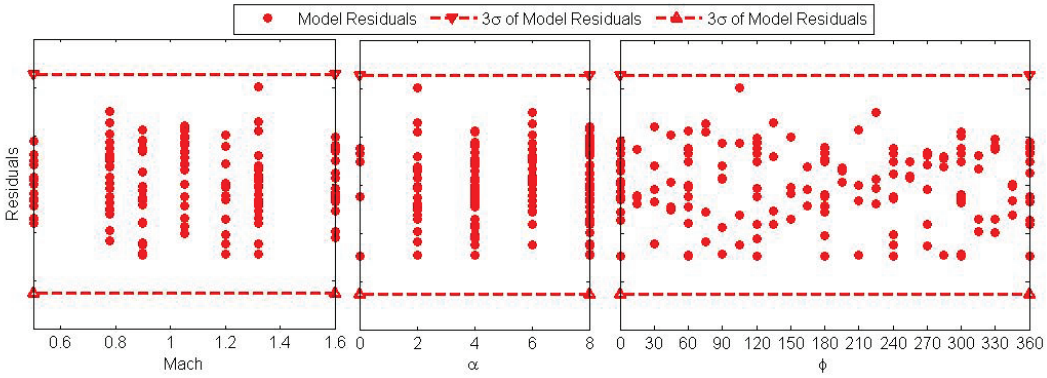

Figure 23: Residuals with validation points included during modeling.

Referring back to the discussion of Model A and Model B, B including the observation values and A not including them, the final product for this dataset would most likely include the validation points while retaining the error associated with predicting the validation points. This would include all relevant information and retain a good estimate of prediction error within the area of operation. This method allows for constant and easy model and error updating when new data becomes available.

G. Lessons Learned and Future Work

All values at $\alpha_T = 0°$ were applied across roll, i.e., the value at $\varphi = 0°$ is the constant value across all values of φ for that Mach number. This seems to gain efficiency in the data matrix because only one CFD run is taken for all roll values at zero α_T. But, this creates very large derivative changes between $\alpha_T = 0°$ and $\alpha_T = 2°$, where the response is very nonlinear. This is problematic because the surface has to "catch up" to the nonlinearities or smooth to a constant value at $\alpha_T = 0°$. In future studies, $\alpha_T = 0°$ values will be taken in addition to values at incidence, as a separate design. Because so few are required, it will not impact the efficiency of the design. The next design should contain an incidence range of 2 to 8°. Much diligence should be taken to ensure that all points in the design space are taken at the exact values as requested, in order to guard against multicollinearity and protect the prediction capabilities of the response surfaces.

Jet efficiency should be evaluated, in addition to the rolling moment variable in this study, in the same fashion. The efficiency factor could be much less complex and require less complex modeling. If this is the case, a sequential test schedule, using efficiency factor as the main response, could result in a dramatically reduced test matrix.

The use of non-parametric modeling algorithms should be evaluated and compared to the results of this study. Methods such as Kriging interpolation and radial basis functions were not available for this work but could have proven more successful than the LS methods studied here.

V. Conclusion

The application of DOE/RSM to highly nonlinear aerodynamics characterization problems can be done well using some of the techniques presented in this work. All models except for the multiple sector, characterized the data adequately. The downfall for the multiple sector analysis was the missing bounding data points in sector 2, highlighting the sensitivity of the approach to missing data. This approach could still be employed in the future if all requested observations are available, as most individual sectors performed very well. The goodness of fit values of each approach are summarized in Table 3. It is apparent from this comparison that the multiple sector approach performed almost as well as the recursive weighted approach except for the prediction R^2 values. The single regression model is the easiest to perform and evaluate. This model can also be optimized more readily as there is only one function to define it. In cases where model accuracy of 93–95% is acceptable, this would certainly be the desired approach. The continuous sector approach performed adequately, but the addition of complexity did not gain much benefit over the single model. However, combining the continuous sector method with recursive weighting and response surface observations provided the most accurate and usable models, as the inclusion of true values did not induce large derivative changes that are undesired. This approach has promise for use in wind tunnel testing as well; where individual point goodness can be used to weigh replicates. The model can be updated in-situ as each new point is taken until a tolerance in prediction or some other factor has been obtained. A similar type of in-situ dynamic modeling has been applied effectively and accurately to flight test data by Morelli and Smith[23]. An extension to ground testing should be natural. The application of robust criterion and influence functions will also expand the application of DOE/RSM to highly nonlinear systems.

Table 3: Goodness of fits.

Goodness of Fit	Single	Multiple	Continuous	Recursive Weighted
R^2	0.949	0.981	0.965	0.981
Adjusted R^2	0.943	0.970	0.960	0.978
Prediction R^2	0.935	0.938	0.964	0.980

The application of these types of experiment designs and modeling schemes can be used in deterministic systems as well as those with systematic and random errors. The gain in efficiency of orthogonal arrays can be effective in reducing design cycle time and resource needs while gaining more information per individual observation than can be accomplished in traditional test methods.

Acknowledgments

The author thanks the NASA Langley Research Center Ares Project Office for supporting this effort with funding and supplying data under the LASER BPA 9009-086 contract. The author thanks Dr. Paul Pao, Dr. Michael Hemsch, and the Technical Monitor Bandu Pamadi of the Ares I Aerodynamics Team for fruitful discussion on this topic.

References

[1]DeLoach, R., "Assessment of Response Surface Models Using Independent Confirmation Point Analysis," AIAA Paper 2010–741, 2010.

[2]DeLoach, R., "Bayesian Inference in the Modern Design of Experiments," AIAA Paper 2008–847, 2008.

[3]DeLoach, R., Rayos, E., Campbell, C., Rickman, S., Larsen, C., "Space Shuttle Debris Impact Tool Assessment Using the Modern Design of Experiments," AIAA Paper 2007–550, 2007.

[4]Landman, D., Simpson, J., Vicroy, D., Parker, P., "Efficient Methods for Complex Aircraft Configuration Aerodynamic Characterization using Response Surface Methodologies," AIAA Paper 2006–922, 2006.

[5]Landman, D., Simpson, J., Mariani, R., Ortiz, F., Britcher, C., "Hybrid Design for Aircraft Wind-Tunnel Testing Using Response Surface Methodologies," *Journal of Aircraft*, Vol. 44, No. 4, July–Aug 2007, pp. 1214–1221.

[6]Favaregh, N., Landman, D., "Global Modeling of Pitch Damping from Flight Data," AIAA Paper 2006–6145, 2006.

[7]Parker, P., Morton, M., Draper, N., Line, W., "A Single-Vector Force Calibration Method Featuring the Modern Design of Experiments," AIAA Paper 2001–0170, 2001.

[8]Parker, P., Finley, T., "Advancements in Force and Attitude Calibration by Integrating Response Surface Methodology and Statistical Quality Control," AIAA Paper 2005–7603, 2005.

[9]Rhew, R., Parker, P., "A Parametric Geometry Computational Fluid Dynamics (CFD) Study Utilizing Design of Experiments (DOE)," AIAA Paper 2007–1615, 2007.

[10]Gnemmi, P., and Schäfer, H., "Experimental and Numerical Investigations of a Transverse Jet Interaction on a Missile Body," AIAA Paper 2005–52, 2005.
[11]Ebrahimi, H., "Numerical Investigation of Jet Interaction in a Supersonic Freestream," *Journal of Spacecraft and Rockets*, Vol. 45, No. 1, Jan–Feb 2008, pp. 95–103.
[12]Dickmann, D., Lu, F., "Jet in Supersonic Crossflow Over a Flat Plate," AIAA Paper 2006–3451, 2006
[13]Srivastava, B., "Computation and Validation of Asymmetric Force and Moment Coefficients for Lateral Jet Controlled Supersonic Missile," AIAA Paper 1998–2410, 1998.
[14]Praharaj, S., Roger, R., Chan, S., Brooks, W., "CFD Computations to Scale Jet Interaction Effects from Tunnel to Flight," AIAA Paper 1997–0406, 1997.
[15]Seiler, F., Gnemmi, P., Ende, H., Schwenzer, M., Meuer, R., "Jet Interaction at Supersonic Cross Flow Conditions," *Shock Waves*, Vol. 13, May 2003, pp. 13–23.
[16]Dickmann, D., Lu, F., "Shock/Boundary Layer Interaction Effects on Transverse Jets in Crossflow Over a Flat Plate," AIAA Paper 2008–3723, 2008.
[17]Fagin, S., Bauer, R., "Aerodynamic Characteristics of a Jet Controlled Projectile," AIAA Paper 1983–0392, 1983.
[18]NASAfacts, "Constellation Program: America's Fleet of Next-Generation Launch Vehicles", http://www.nasa.gov/pdf/366590main_Ares_I_FS.pdf, retrieved April 1, 2010.
[19]Montgomery, Douglas C., *Design and Analysis of Experiments*. 5th Edition. New York: John Wiley & Sons, 2001.
[20]Frink, Neal T., TetrUSS USM3D: Home Page, http://tetruss.larc.nasa.gov/usm3d/, last access May 26, 2010.
[21]Buning, Pieter G., Pieter G. Bunning's Home Page: "Overset Grid CFD Software," http://aaac.larc.nasa.gov/~buning/, last access May 26, 2010.
[22]Myers, Raymond H., and Douglas C. Montgomery, *Response Surface Methodology: Process and Product Optimization Using Designed Experiments*. 2nd Edition. New York: John Wiley & Sons, Inc., 2002.
[23]Morelli, E., Smith, M., "Real-Time Dynamic Modeling: Data Information Requirements and Flight-Test Results," *Journal of Aircraft*, Vol. 46, No. 6, Nov–Dec 2009, pp. 1894–1905.